

# Extended NVNA Bandwidth for Long-Term Memory Measurements\*

Kate A. Remley<sup>1</sup>, *Member, IEEE*, Dominique M. M.-P. Schreurs<sup>2</sup>, *Senior Member, IEEE*, Dylan F. Williams<sup>1</sup>, *Fellow, IEEE*, John Wood<sup>3</sup>, *Senior Member, IEEE*

1. National Institute of Standards and Technology 818.01, 325 Broadway; Boulder, CO 80305
2. Katholieke Universiteit Leuven, Div. ESAT-TELEMIC, Leuven, Belgium
3. Agilent Technologies; Santa Rosa, CA

**Abstract** — We present a new technique for measuring the magnitude and phase of intermodulation products outside the measurement bandwidth of our instrumentation. We apply the technique to measurements of long-term memory, and relate our measurements to frequency-dependent physical characteristics of the circuitry.

**Index terms** — Intermodulation distortion, long-term memory, nonlinear vector network analyzer.

## I. INTRODUCTION

Nonlinear vector network analyzers (NVNAs) [1] were developed to provide calibrated measurements of the magnitude and phase of periodic signals at the input and output ports of nonlinear circuits and systems. When coupled with a post-processing phase alignment routine [2], the NVNA can simplify vector calibrated measurements of intermodulation (IM) products. Since the measurements are provided directly, they are easier to perform than the methods presented in Refs. [3-7].

As discussed in Refs. [8,9], NVNAs utilize sampling frequency converters to map the frequency components of radio-frequency (RF) signals (including discrete-tone modulation and harmonics) to a set of calculable intermediate frequencies (IF). A careful choice of the measurement frequency grid and sampling frequency allows for the measurement of many RF frequency components simultaneously.

To correct for distortion introduced by the downconversion process, current NVNA systems either fix the downconversion bandwidth and perform an IF calibration over this limited frequency range, or use one of the four downconverted wave variables as an ideal reference for the other three [9]. We can circumvent the difficulties associated with these methods by using an external alignment of the phases of a discrete-tone modulated signal outside the default IF bandwidth of our NVNA. No assumption is made regarding the ideality of the downconversion of any of the wave variables. We demonstrate the utility of our new measurement technique by considering long-term memory effects acting on a high-electron mobility transistor (HEMT) transistor.

## II. LONG-TERM MEMORY MEASUREMENTS

Long-term memory is often characterized by a variation in the magnitude and phase of the IM products as frequency spacing is changed. Long-term memory may be caused by physical mechanisms including thermal heating, electron trapping, and impact ionization, as well as electrical effects due to the frequency response of bias circuitry and other terminations.

To demonstrate measurements using the NVNA, we consider an on-wafer 0.15  $\mu\text{m}$  x 100  $\mu\text{m}$  GaAs-based metamorphic HEMT (MHEMT) excited by a two-tone signal and biased for maximum gain. We sweep both input voltage level and frequency spacing to characterize the device's long-term memory behavior. Because the device is of small size, we do not expect significant heating or power dissipation that would cause long-term memory due to thermal effects.

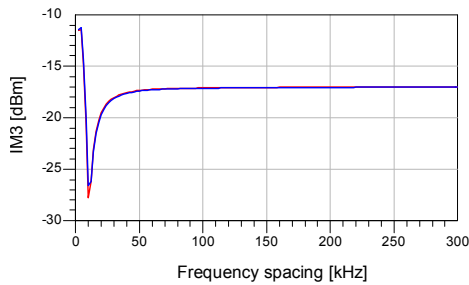
However, the response of the bias circuitry may significantly affect the IM response of our device. We first consider a bias network that does not induce long-term memory over a broad frequency range. Figure 1 shows the simulated response of a simple FET model embedded between two such bias networks. We represent these bias networks by an equivalent circuit consisting of a series capacitance, parallel inductance and series resistance taken from the manufacturer's specifications. Note the spike in the IM3 response in the 5-10 kHz range.

Standard NVNA measurements of the IM3 products of the MHEMT device using this bias circuit are shown in Figs. 2(a) and (b), where we aligned the phase measurements using the procedure in Ref. [2]. Note that variation in the magnitude and phase response also occurs in the 5-10 kHz range as well.

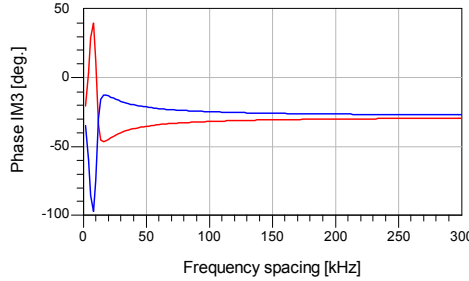
Figure 3 shows the IM3 response of the same simulated FET circuit, but using the manufacturer's component values for a bias tee whose components induce long-term memory over a much broader frequency range. To completely characterize long-term memory effects due to this bias circuit, we need to use wider two-tone frequency spacings than normally possible with our NVNA because of its 8 MHz IF bandwidth limitation.

---

\* Partial work of the U.S. Government, not subject to copyright.

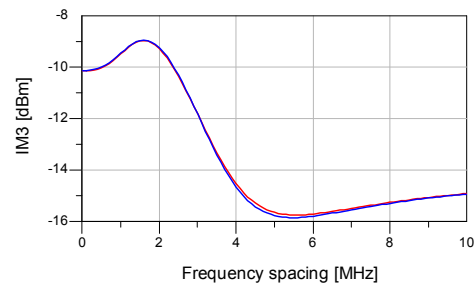


(a)

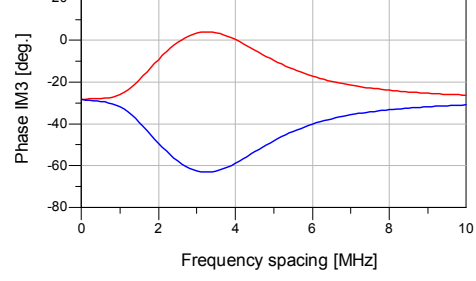


(b)

**Fig. 1:** Simulation of a FET device with a bias tee that induces long-term memory over a narrow frequency range. The plot shows (a) magnitude and (b) phase values of the IM3 products as a function of frequency. Lower IM3 product is red, upper IM3 product is blue. Bias circuit values were taken from manufacturer's specifications.

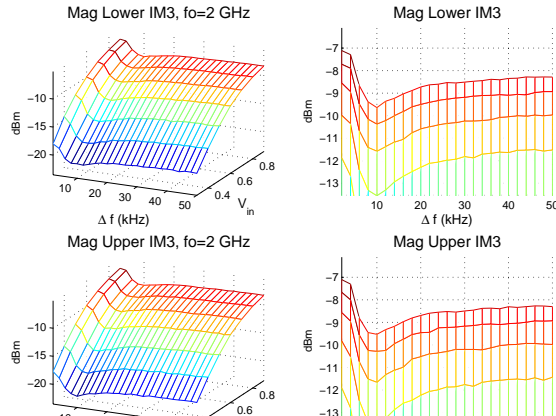


(a)

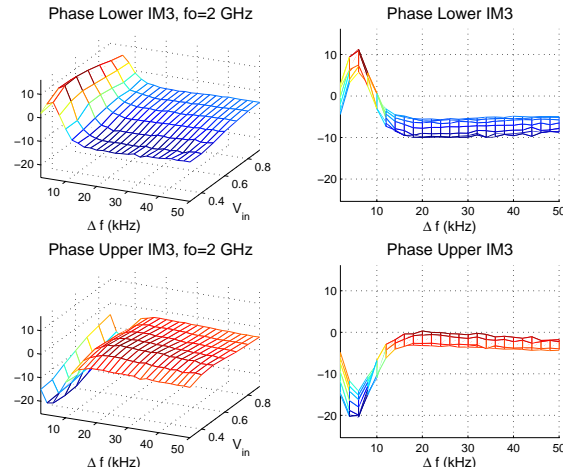


(b)

**Fig. 3:** Simulation of a FET device with a bias tee that induces long-term memory over a broad frequency range. The plot shows (a) magnitude and (b) phase values of the IM3 products as a function of frequency. Lower IM3 product is red, upper IM3 product is blue. Bias circuit values were taken from manufacturer's specifications.



(a)



(b)

**Fig. 2:** Two views each of (a) magnitude and (b) phase (in degrees) of the IM3 products at the output of an MHEMT device with sweeps of both input voltage and frequency spacing of the two-tone excitation. Variation in the magnitude and phase with frequency spacing indicates the presence of long-term memory effects. Here the device was biased using the same bias tee as was used for the data of Fig. 1, and we see the effects of long-term memory for narrow frequency spacings. Note that the phase of the IM3 upper and lower are nearly identical, but of opposite sign, as expected for baseband long-term memory effects [3, 4, 6].

### III. DEVELOPMENT OF THE MEASUREMENT METHOD

Our method to measure IM products that lie outside our 8 MHz measurement bandwidth is based on a series of calibrated single-frequency NVNA measurements at each excitation tone and IM product frequency, as illustrated in Fig. 4. While NVNA calibrations make this a straightforward technique for magnitude measurements, phase alignment is somewhat more complicated.

A common way to align the phase components of a multi-frequency signal is to provide a calibration signal with known phase relationships [1-3]. Here, our calibration signal consists of a set of small “tickler” tones generated at the input of the circuit (shown by the small solid arrows in Fig. 4). Ticklers are generated at the IM frequencies along with the large-signal two-tone excitation. We specify the phase of each tone of the input signal on our vector signal generator. We can determine the IM product phases from the relative input-to-output phase measured by the NVNA and the known phases of the input signal.

We can implement our IM-product phase-alignment procedure in three steps: first, we calculate the frequencies of all IM products of interest and perform a separate NVNA calibration at each. Thus, for every two-tone frequency spacing, we would need six calibrations to measure the two excitation tones, the two IM3 products, and the two IM5 products.

The second step is to load the calibration corresponding to one of the IM products, apply the two-tone excitation, and apply a tickler at that IM product frequency. We measure the phase of the output signal (tickler + IM product) at that frequency, relative to the known input phase. Note that we apply only one tickler at a time to minimize the effects of image-frequency mixing inherent in any nonlinear device measurement [10].

The third step is to externally correct the output response for the presence of the amplified tickler. To do this, we approximate the small-signal transfer function of the device by applying only the two-tone excitation at each desired input voltage level and measure the output response of one of these tones. We apply this transfer function to the measured input tickler and subtract the result from the measured output. Note that to correctly find the small-signal transfer function of the device under large-signal excitation, we would need to apply a linearization technique such as that described in Ref. [10]. For simplicity, we approximate the transfer function of the device, as above.

Our procedure is based on two assumptions: that the relative phases generated by the vector signal generator are in fact those we specified, and that the tickler is the only signal present at the input of the DUT at the IM

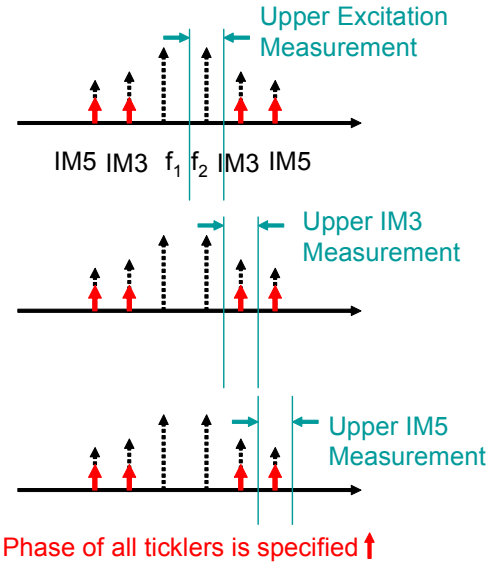


**Fig. 4:** Overview of the measurement procedure used to extend the bandwidth of the NVNA in order to measure IM products. The dashed lines represent the individual measurements of the two-tone signal and the IM products. The dotted lines with arrows represent the measured quantities. The small solid lines represent the tickler tones used to align the phases from measurement to measurement.

product frequencies. We validated both of these assumptions, at least to the first order, with calibrated oscilloscope measurements of multisine signals from the generator and through comparative measurements of the amplifier with and without the ticklers present. The verification presented in the next section provides further support of the assumptions above.

### IV. BROADBAND TWO-TONE MEASUREMENT RESULTS

We first wished to confirm that our procedure provides IM product measurements with the same accuracy as our standard NVNA modulated-signal measurement procedure. To accomplish this, we performed measurements of a two-tone signal whose IM3 and IM5 products fell inside the NVNA’s IF bandwidth.

The fundamental frequency for this measurement was 2 GHz, the two-tone frequency spacing was 1 MHz, the amplitude of each of the two excitation tones was 0.8 V (an input level high enough to drive the device well into its nonlinear state). We specified the relative phase of all frequency components to be 0° on our signal generator.

For this measurement, we chose a tickler amplitude of 0.025 V, or about -22 dBm. This signal is low enough as not to influence the large-signal gain, but high enough to be well above our measurement noise floor of approximately -70 dBm. Agreement was virtually identical in magnitude and was within 2° in phase for the IM3 product levels, and within 8° in phase for the IM5

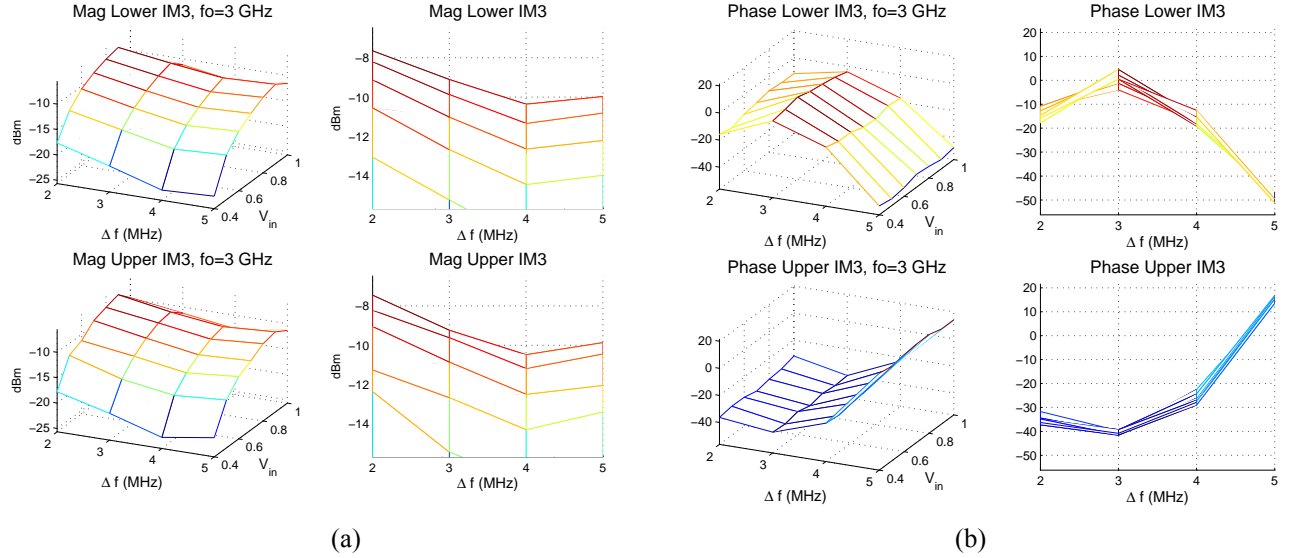


**Fig. 5:** NVNA measurements made using the new broadband technique of (a) magnitude and (b) phase (in degrees) of the IM3 products for the MHEMT using the bias tee whose response is given in Fig. 3. Note that the frequency spacing of the excitation tones is much broader, and that the spacing of the IM products is much greater than 8 MHz.

products. The larger discrepancy for the IM5 products is not surprising. Due to their lower level they are more susceptible to system noise.

Having verified the method, we next applied it to the MHEMT device with the bias tee whose simulated IM3 response is shown in Fig. 3. We swept the input voltage from 0.4 to 1.0 V and the two-tone frequency spacing from 2 to 5 MHz, producing IM3 products spaced from 6 to 15 MHz. The magnitude and phase of the measured IM3 products are shown in Figs 5(a) and 5(b), respectively. Due to the bias tee's broad long-term memory effect, we expect to see variation in magnitude and phase of the IM products at wider frequency spacings. These effects are readily apparent in our measurements as the two-tone frequency spacing is increased.

## V. CONCLUSION

We introduced a new technique for increasing the measurement bandwidth of NFNAs that have fixed IF bandwidths for two-tone measurements. The method involves performing successive calibrations and measurements, centered at the frequency of each IM product. Small phase-alignment tones are measured and subsequently corrected for. We showed that this method works as well as the standard NVNA modulated-signal procedure, and demonstrated that broadband long-term memory effects may be identified using the additional measurement bandwidth. Note that our method does not require the assumption of ideality of one downconverted channel and does not require the use of the NVNA's IF calibration.

## REFERENCES

- [1] T. Van den Broeck and J. Verspecht, "Calibrated vectorial nonlinear-network analyzers", *IEEE Int. Microwave Symp. Digest*, 1994, pp. 1069-1072.
- [2] K.A. Remley, D.F. Williams, D. Schreurs, G. Loglio, and A. Cidronali, "Phase Detrending for Measured Multisine Signals," 61<sup>st</sup> Automatic RF Techniques Group Conference (ARFTG), pp. 73-83, 2003.
- [3] J.H.K. Vuolevi, T. Rahkonen and J.P.A. Manninen, "Measurement technique for characterizing memory effects in RF power amplifiers," *IEEE Microwave Theory Tech.*, Vol. 49, no. 8, Aug. 2001, pp. 1383-1389.
- [4] N. Borges de Carvalho and J.C Pedro, "A comprehensive explanation of distortion sideband asymmetries," *IEEE Microwave Theory Tech.*, Vol. 50, no. 9, Sept. 2002, pp. 2090-2101.
- [5] H. Ku, M.D. McKinley, and J.S. Kenney, "Quantifying memory effects in RF power amplifiers," *IEEE Trans. Microwave Theory Tech.*, vol. 50, no. 12, Dec. 2002, pp. 2843-2849.
- [6] J. Brinkhoff and A.E. Parker, "Effect of baseband impedance on FET intermodulation," *IEEE Microwave Theory Tech.*, Vol. 51, no. 3, Mar. 2003, pp. 1045-1051.
- [7] J. Dunsmore and D. Goldberg, "Novel two-tone intermodulation phase measurement for evaluating amplifier memory effects," 33<sup>rd</sup> European Microwave Conf., Oct. 2003, pp. 235-238.
- [8] P. Crama and Y. Rolain, "Broad-band measurement and identification of a Wiener-Hammerstein model for an RF amplifier," 60<sup>th</sup> Automatic RF Techniques Group Conference (ARFTG), pp. 49-57, 2003.
- [9] J. Verspecht, "The return of the sampling frequency converter," 62<sup>nd</sup> Automatic RF Techniques Group Conference (ARFTG), pp. 155-161, 2004.
- [10] J. Verspecht, M. Vanden Bossche, and F. Verbeyst, "Characterizing components under large signal excitation: defining sensible 'large signal S-parameters'!?", 49<sup>th</sup> Automatic RF Techniques Group Conference (ARFTG), pp. 109-117, 1997.